

## MICROSTRUCTURE AND PROPERTIES OF HEAT-AFFECTED HVOF SPRAYED HASTELLOY C-276 COATING

HOUDKOVÁ Šárka<sup>1</sup>, VOSTRÁK Marek<sup>1</sup>, ČESÁNEK Zdeněk<sup>1</sup>, GLANC Aleš<sup>1</sup>, SMAZALOVÁ Eva<sup>1</sup>

<sup>1</sup>University of West Bohemia, Pilsen, Czech Republic, EU

[houdkov@ntc.zcu.cz](mailto:houdkov@ntc.zcu.cz)

### Abstract

The influence of heat treatment on the microstructure, mechanical and sliding wear properties of Hastelloy C-276 HVOF sprayed coatings was evaluated. The applied furnace heat treatment modified the coatings microstructure, leading to precipitation hardening and oxidation of inter-splat boundaries, but had a negative effect on the sliding wear resistance. The laser heat treatment eliminated the intersplat boundaries and porosity. The obtained dendritic microstructure have lower microhardness compare to as sprayed coating, which implies higher toughness possibly being beneficial to avoid the brittle fracture during wear loading.

**Keywords:** Hastelloy C-276, HVOF, laser remelting, heat treatment, mechanical properties

### 1. INTRODUCTION

In the most challenging branches of industry, such as power generation or aerospace, the components are exposed to the combination of high temperature, aggressive environment and mechanical load. Only materials with superior properties, such as highly-alloyed steels or super alloys can be applied in such environments. Appropriately to their material composition, the price of components is high. The material costs can be reduced by application of surface protective layers, offering the sufficient functional properties while preserving the lower-cost components body. Among other surface treatment technologies, the thermal spray technology, namely High Velocity Oxy-Fuel (HVOF) spraying, is a suitable for applying hard, wear and oxidation resistant coatings onto the surface of less noble steels. The Ni-based superalloys are generally known for their high corrosion resistance in various kinds of environment, including the high temperature. As a thermally sprayed coating, they are used namely in chemical, aerospace or power industry. There are several Ni-based superalloys, generally based on the Ni-Cr solid solution. In dependence on the type and amount of other alloying elements, the high temperature strength, wear or corrosion resistance are varied. In thermal spray community, the self-fluxing wear resistant NiCrBSi alloy is well known and wide-spread [1] [2]. The group of so-called Inconel alloys includes Ni-Cr based alloys with a variable amount of Fe, Mo, Co and Nb elements, responsible for solid solution strengthening or precipitation hardening through intermetallic phases or carbides [3] [4]. The Ni-Cr-Mo alloy, known as Hastelloy® C-276 or just C-276 alloy with the addition of Fe and W is designed to have superior corrosion resistance in the wide range of environments. The high content of Mo (16%) is responsible for high pitting corrosion resistance in reducing environments, while C (16%) makes the alloy resistant in oxidizing media. Compare to other Ni-based alloys, the carbon content is kept low to avoid the carbide grain boundary precipitation during welding, responsible for lowering the corrosion resistance and deterioration of mechanical properties. However, the studies exists [5] describing the second phase particles precipitating in Hastelloy -276 alloy as a result of thermal treatment above 650°C, having the form of intermetallic phases  $\mu$  and P (A7B6)  $M_6C$  carbide, despite low carbon content. Usually, the intermetallic phases are considered to play a negative role, being responsible for weld metal hot cracks in Hastelloy C-276 as well as for deterioration of its corrosion resistance. To avoid their precipitation, the fast cooling processes, such as electron beam or laser beam welding can be applied [6]. Laser surface treatment of bulk Hastelloy C-276 was carried out in [7] at different laser process parameters to improve the material wear resistance through refining the microstructure without undesirable precipitation. On the other hand, the precipitation was used for strengthening of the Ni-based coatings with a composition similar to Hastelloy C-276. In [8] the C-276 coating

deposited by magnetron sputtering was analyzed. Compare to the bulk material, the fine-grained coatings microstructure was much harder, and the hardness further increased through segregation and precipitation of Cr and Mo rich regions during thermal treatment. The thermally sprayed coatings microstructure differs usually from the microstructure of bulk material not only due to its lamellar character but also due to the high cooling rates during solidification. It can lead to a creation of unstable phases, as well as amorphous or nanocrystalline structures. Their application in high temperature environment can lead to microstructural changes, which can influence the coatings mechanical behavior. Based on above mentioned studies, the effect of such changes can be both - negative or positive. The aim of the study is to evaluate the effect of heat treatment on the HVOF sprayed Hastelloy C-276 on coatings mechanical properties and tribological behavior. To cover both possibilities, the two types of heat treatment was applied: i) the age hardening at 600°C for 116 h to observe the potential precipitation and ii) laser surface remelting with high cooling rates to suppress the precipitation, but eliminate the defects of thermal sprayed coatings microstructure.

## 2. EXPERIMENTAL

### 2.1. Coatings deposition

The Hastelloy C-276 coating was sprayed by HP/HVOF TAFA JP5000 spraying equipment in VZU Plzen onto grit blasted 11 523 substrate. For spraying, the FST 341.33 powder was used. Its nominal chemical composition is: 15.5%Cr; 15.5%Mo; 4%W; 3%Fe; Ni rest. The maximal content of C in Hastelloy C-276 is expected not to exceed 0.01%. The grit blasting was realized by Al<sub>2</sub>O<sub>3</sub>, F22 (with a grain size 0.8-1 mm). For laser treated samples, the dimensions of the substrate (200 x 100 x 10 mm) were chosen to ensure sufficient heat dissipation during laser remelting process. The annealing process was carried out in air atmosphere in muffle furnace (LM 212), at 600°C for 116 hours. The samples were then cooled in air. The non-coated parts of steel samples were protected against oxidation by oxidation protective paint CONDURSAL Z 1100. The HPDD 4kW laser Coherent HighLight ISL-4000L; 808 ± 10 nm wavelength was used for laser re-melting. Based on the experimental process, two sets of parameters (denominated as LR1 and LR2) were chosen: The fluence 8.9 J/mm<sup>2</sup> and 17.8 J/mm<sup>2</sup>, traverse speed 10 mm/s and 5 mm/s, spot size 12 x 1 mm, 2 mm overlap. To prevent the high thermal gradient, responsible for cracking of the coating, the pre-heating of the substrate to the 350°C was used. After remelting, the samples were cooled in air.

### 2.2. Coatings characterization

The microstructure of as-sprayed and annealed coatings were evaluated by optical microscope on cross sections (ground and polished by automatic Leco grinding and polishing equipment) by digital optical 3D microscope Hirox KH7700, and SEM Quanta 200 from FEI. The microhardness depth-profiles were evaluated by HV0.1 measurement for both as-sprayed and annealed coating. The indents were made in 100 µm distant steps, starting 50 µm below the coatings surface. Six indents were made in each depth, the average value is reported. The mechanical properties of as-sprayed and furnace-annealed coatings were measured also by NanoTest Vantage (Micro Materials) nanohardness tester equipped with Berkovich indenter loaded with loads 100 mN and 300 mN, respectively with loading and unloading time of 30 s each and 10 s dwell period under the load. The measurement was conducted on polished cross-section of the sample under room temperature. Values of hardness H and effective Young's modulus E\* were calculated from 15 measurements in line approximately in the middle of the sprayed coating. The distance between the measurements was 15 µm to ensure that measurements did not affect each other. Coatings' phase composition was evaluated and compared by means of X-ray diffraction (XRD), using the D8 Discover powder diffractometer in Bragg-Brentano geometry with 1D detector and CoK $\alpha$  radiation (scanned region from 20 to 100 °2 $\theta$  with 0.03 °2 $\theta$  step size and 96 s counting time per step). The obtained diffraction patterns were subjected to quantitative Rietveld analysis [9] performed in TOPAS 4.2 which uses the so-called fundamental parameters approach [10]. In this manner, we analyzed (i) feedstock powder, (ii) the surface in the as-sprayed state, (iii) the surface

of annealed coating in as-received and ground state in order to identify the formed oxides in surface oxide layer together with potential changes of phase composition inside the coatings. The sliding wear resistance and coefficient of friction (COF) of as-sprayed coating were evaluated at room and elevated (600°C) temperatures, the annealed coating behavior was evaluated at room temperature. The laser remelted coatings sliding wear behavior is not reported in this study but will be a subject of the following work. The parameters of the Ball-on-Flat test (ASTM G133) were as follows: 25 N Load; steel100Cr6, 6 mm diameter ball counterpart; 5 Hz oscillating frequency; 10 mm stroke length; 1000 s testing time. For each coating, three different measurements were performed. The wear tracks profiles were measured by profilometer KLA-Tencor P-6 Profiler, at three different places, and the wear volume was calculated. Prior to sliding wear tests, the surface of the coating was ground and polished to the  $0.04 \pm 0.02$  Ra value. Both the abrasive and adhesive wear was characterized by the coefficient of wear K [ $\text{mm}^3/\text{Nm}$ ], calculated from the coating volume loss, used load and the abrasive or sliding distance. After the tests, the SEM of wear track was observed, to identify the wear mechanism.

### 3. RESULTS AND DISCUSSION

#### 3.1. Microstructure

There were no cracks in the coating or delamination between coating and substrate observed for as-sprayed and furnace-annealed coatings (**Figure 1**). For both coatings, a certain amount of porosity was recorded, as well as decohesion between individual splats. Inside the splats, the very fine dendritic microstructure can be seen. The XRD analyses confirm the presence of  $\gamma$  phase (Ni-based solid solution) only in the original powder and in the as-sprayed coating. In the furnace-annealed coating, the precipitation of  $\text{M}_6\text{C}$  carbide, most probably  $\text{Fe}_3(\text{Mo,W})_3\text{C}$  was recorded in the amount of ca 10% wt. according to Rietveld analyses. As a result of oxidation, NiO (2.9% wt.) and  $\text{Mo}_3\text{O}$  (1.2% wt.) oxides created on the surface of the furnace-annealed coating were observed. After surface grinding the 0.1%wt of  $\text{Mo}_3\text{O}$  was still present, confirming oxidation of intersplat boundaries. Nevertheless, the newly created phases,  $\text{M}_6\text{C}$  carbide and the intersplat oxides, was not found during SEM cross sections analyses due to the low content of both.

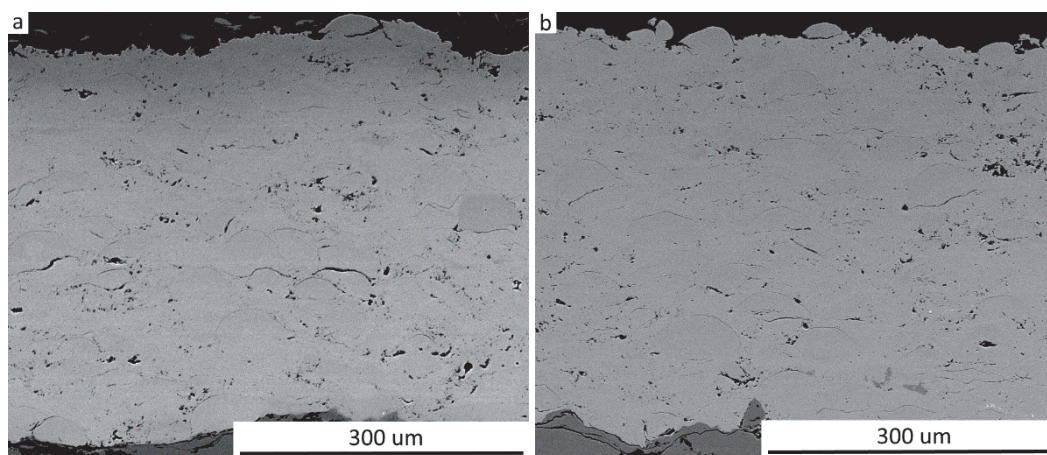


**Figure 1** Microstructure of HVOF as-sprayed C-276 coating (a) and furnace annealed coating (b)

The laser remelting procedure led to significant modification of coatings microstructure (**Figure 2**). Due to the shrinkage of the coating during fast solidification, the cracks appeared for both used laser treatment parameters, despite the application of substrate preheating.

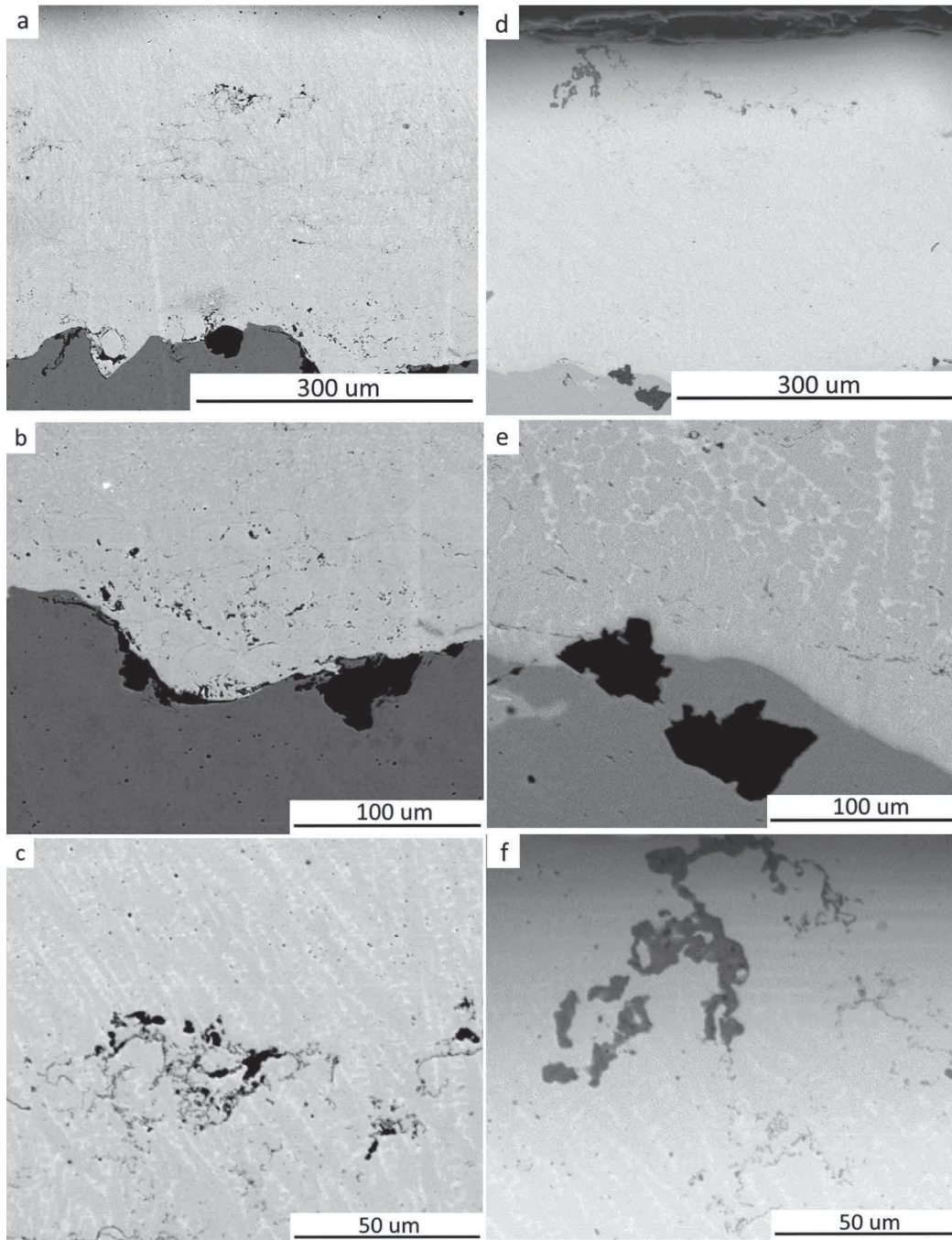


**Figure 2** Microstructure of laser remelted coatings by lower (a,b,c) and higher (d,e,f) laser energy specific density

The problem of cracking during laser treatment of preplaced coatings or laser cladding of Ni-based alloys is more complex, including not only the materials thermal properties but also the presence of elements, increasing the material sensitive hot cracking susceptibility [11]. Based on the applied fluence, the depth of re-melting differs [12]. The splats, typical for as-sprayed coatings were replaced by dendritic microstructure, significantly coarser than the fine dendrites inside the splats. In the LR1 coating, the original as-sprayed microstructure was preserved near the coating-substrate boundaries (**Figure 2b**). In LR2 coating, full coating thickness was remelted, together with a thin layer of substrate material. The beneficial metallurgical bonding between coating and substrate was confirmed by EDX analyses, showing increased amount of Fe in the coating near the coating-substrate boundary. Even though the microstructure of laser remelted coatings is

much more homogenous than as-sprayed, still it contains some imperfections. In the LR1 coating, some of the original porosity still remains, changing its morphology to clusters (**Figure 2c**). The LR2 coating contains significantly less porosity and other inhomogeneity. The less frequent, but larger pore clusters had the tendency to flow up toward the surface. Inside them, the empty space was replaced by oxides (**Figure 2f**).

### 3.2. Mechanical properties

The microhardness depth profiles can be seen in the graphs in the **Figure 3a**. Obviously, the furnace annealed coatings microhardness increased compare to as-sprayed coating. It could be an effect of precipitation hardening as well as the presence of oxides on the intersplat boundaries, both of which can contribute to the hardening of the Ni-based solid solution. The change of mechanical properties was further confirmed by nanohardness evaluation. The hardness increased from  $5.4 \pm 0.2$  GPa to  $6.0 \pm 0.5$  GPa and from  $3.0 \pm 0.6$  GPa to  $5.6 \pm 0.4$  GPa for 100 mN and 300 mN respectively. The effective Young's modulus  $E^*$  increased from  $155 \pm 6$  GPa to  $176 \pm 8$  GPa and remained almost the same  $160 \pm 4$  GPa vs  $165 \pm 4$  for 100 mN and 300 mN resp. The higher increase of hardness recorded for higher load implies, that the presence of oxides at the intersplat boundaries plays the more dominant role compared to precipitation hardening of in-splat Co-based solid solution. On the other hand, the increase of  $E^*$  at lower loads showed on some change of in-splat resistance to plastic deformation. In [13], the increase of HV0.1 of Co-Mo-Cr alloy in the vicinity of 600°C heat treatment is also reported, accompanied by the increase of Young's modulus. On the contrary, the microhardness of laser remelted coating decreased significantly, no matter the applied laser energy specific density. The microhardness of the substrate was also influenced by heat treatment, more intensively for furnace long-term annealing.

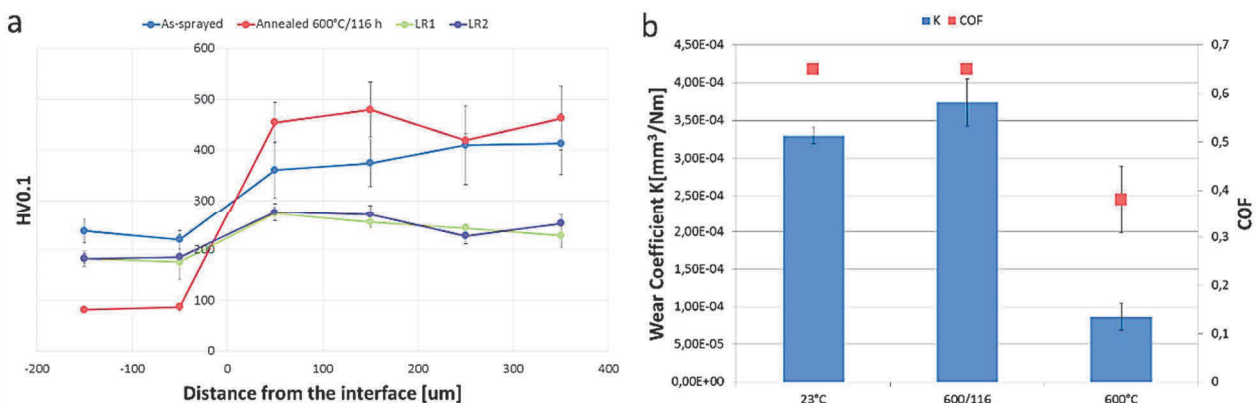


**Figure 3** Microhardness depth profile (a) and Coatings Wear coefficient and Coefficient of Friction (b)

### 3.3. Sliding wear behavior

The sliding wear behavior of as-sprayed coating at room and elevated temperature and the furnace-annealed coating at room temperature are summarized in the **Figure 3b**. It can be seen, that the wear rate of furnace-annealed coating decreased in spite of the increase of microhardness. The SEM analyses of wear mechanism show the presence of brittle cracking in the wear track of furnace-annealed coating, confirming the assumption of negative influence of precipitation in Hastelloy C-276 coating. On the other hand, the wear rate, as well as the coefficient of friction measured at elevated temperature, is significantly lower. In the wear track, the oxide layer as a result of tribooxidation was identified. Usually, the high temperature sliding tests result in higher wear rates due to the softening of the material and making it more prone to plastic deformation [13]. In the case of Hastelloy coating, the less plastic deformation is present after high temperature sliding wear test, compare to room temperature. The possibility of the positive role of oxide tribofilm comes to one's mind, but need to be further confirmed.

#### 4. CONCLUSION

In the paper, the influence of thermal post treatment on the microstructure and mechanical properties are briefly described. It was showed, that heat exposition of the HVOF sprayed Hastelloy coating can modify the microstructure, leading to precipitation hardening and oxidation of intersplat boundaries. Despite microhardness increase, the microstructural changes had a negative effect on the sliding wear resistance, probably due to the increased brittleness. The laser treatment proved the potential to eliminate the negative intersplat boundaries and porosity, but the coarsening of the dendritic microstructure caused decrease of hardness for both evaluated laser treated coatings. The influence of such treatment on the sliding wear resistance will be further analyzed.

#### ACKNOWLEDGEMENTS

**The research outcome was developed within the project SGS-2016-005. Authors thank Jan Procházka from RTI ZČU for providing of the nanoindentation tests and František Lukáč from IPP AS-CZ for XRD analyses.**

#### REFERENCES

- [1] TRNKOVA, L., GRGAČ, P. Solidification process and microstructure development of the NiCrSiB hard-surfacing alloy, *In: Materials Science and Technology*, 2005, vol. 5, no. 5, ISSN 1335-9053, (in Slovak)
- [2] HOUDKOVÁ, Š., PALA, Z., SMAZALOVÁ, E., VOSTŘÁK, M., ČESÁNEK, Z. Microstructure and sliding wear properties of HVOF sprayed, laser remelted and laser clad Stellite 6 coatings. *Surface and Coatings Technology*, 2016, available on-line, <http://dx.doi.org/10.1016/j.surfcoat.2016.09.012>
- [3] PERRICONE, M.J., DUPONT, J.N. Effect of composition on the solidification behavior of several Ni-Cr-Mo and Fe-Ni-Cr-Mo alloys. *Metallurgical and Materials Transactions A: Physical Metallurgy and Materials Science*, 2006, vol. 37, no. 4, pp.1267-80.
- [4] TANG, X., WANG, S., QIAN, L., LI, Y., LIN, Z., XU, D., ZHANG, Y. Chemical Engineering Research and Design Corrosion behavior of nickel base alloys, stainless steel and titanium alloy in supercritical water containing chloride, phosphate and oxygen. *Chemical Engineering Research and Design*, 2015, vol.100, pp.530-41.
- [5] RAGHAVAN, M., BERKOWITZ, B.J., SCANLON, J.C. Electron Microscopic Analysis of Heterogeneous Precipitates in Hastelloy C-276. *Metallurgical Transactions A*, 1982, vol.13A, pp. 979-984.
- [6] AHMAD, M., AKHTER, J.I., AKHTAR, M. IQBAL, M., AHMED, E., CHOUNHRY, M.A. Microstructure and hardness studies of the electron beam welded zone of Hastelloy C-276. *Journal of Alloys and Compounds*, 2005, vol. 390, no. 1-2, pp.88-93.
- [7] HASHIM, M., SARATH RAGHAVENDRA BABU, K.E., DURAISELVAM, M., NATU, H. Improvement of wear resistance of Hastelloy C-276 through laser surface melting. *Materials and Design*, 2013, vol.46, pp.546-51
- [8] MULLIGAN, C.P., WEI, R., YANG, G., ZHENG, P., DENG, R., GALL, D. Microstructure and age hardening of C276 alloy coatings. *Surface and Coatings Technology*, 2015, vol.270, pp.299-304.
- [9] RIETWELD, H.M. A profile refinement method for nuclear and magnetic structures. *Journal of Applied Crystallography*, 1969, vol.2, no. 2, pp.65-71.
- [10] CHEARY, R.W. A fundamental parameters approach to X-ray line-profile fitting. *Journal of Applied Crystallography*, 1992, vol.25, no. 2, pp.109-21.
- [11] NÄKKI, J., TUOMINEN, J., VUORISTO, P. Effect of minor elements on solidification cracking and dilution of alloy 625 powders in laser cladding. *Journal of Laser Applications*, 2017, vol.29, no.1, pp. 12014-1-7
- [12] VOSTŘÁK, M., HOUDKOVÁ, Š., SMAZALOVÁ, E. Diagnostic of laser remelting of HVOF sprayed Stellite coatings using an infrared camera. *Surface and Coatings Technology*, 2017, available on-line, <http://dx.doi.org/10.1016/j.surfcoat.2016.12.118>
- [13] BOLELLI, G., CANNILLO, V., LUSVARGHI, L., MONTORSI, M., MANTINI, F.P., BARLETTA, M. Microstructural and tribological comparison of HVOF-sprayed and post-treated M-Mo-Cr-Si (M = Co, Ni) alloy coatings. *Wear*, 2007, vol. 263, pp.1397-416.